Vision Research 49 (2009) 2741–2746

Contents lists available at ScienceDirect

Vision Research

journal homepage: www.elsevier.com/locate/visres

Motion-induced position shifts occur after motion integration

George Mather [a,*], Andrea Pavan [b]

[a] Psychology School, University of Sussex, Falmer, Brighton BN1 9QH, UK
[b] Department of General Psychology, University of Padua, Via Venezia 8, 35131 Padua, Italy

ARTICLE INFO

Article history:
Received 1 June 2009
Received in revised form 16 July 2009

Keywords:
Motion perception
Motion-induced position shift
Motion integration

ABSTRACT

Low-level motion processing in the primate visual system involves two stages. The first stage (in V1) contains specialised motion sensors which respond to local retinal motion, and the second stage (in MT) pools local signals to encode rigid surface motion. Recent psychophysical research shows that motion signals influence the perceived position of an object (motion-induced position shift, MIPS). In the present paper we investigate the role played by the two processing stages in generating MIPS. We compared MIPS induced by single grating components (Gabor patches) to MIPS induced by plaids created by combining pairs of components. If motion signals at the lowest level of motion analysis (V1) influence position assignment, MIPS from plaids should reflect the position shift induced by each component when presented separately. On the other hand, if signals generated in MT (or later) influence perceived position, then MIPS from plaids should be consistent with a motion integration computation on the components. Results showed that MIPS from plaids is larger than the MIPS obtained from individual components, and can be explained by the output of an integration process that combines intersection-of-constraints and vector-sum computations.

1. Introduction

Motion processing is believed to involve at least two stages: local detection of motion in striate cortex (V1), and integration of local signals in extrastriate cortical area MT. Motion detection is widely accepted to involve a motion energy computation (Adelson & Bergen, 1985; Pantle & Turano, 1992; Strout, Pantle, & Mills, 1994). A great deal of research on extrastriate motion integration has been conducted using plaids (Fig. 1) created by superimposing two drifting sinusoidal gratings. Results indicate that motion integration involves a combination of different solutions, including intersection-of-constraints (Adelson & Movshon, 1982) and vector-sum (Wilson & Kim, 1994) computations.

Recent psychophysical studies have shown that visual movement influences perceived position (motion-induced position shift, MIPS). In particular, when observing a moving object, its position appears shifted in the direction of motion (Fig. 1) (see Chung, Patel, Bedell, & Yilmaz, 2007; De Valois & De Valois, 1991; Durant & Johnston, 2004; Durant & Zanker, 2009; Edwards & Badcock, 2003; Fang & He, 2004; Fu, Shen, Gao, & Dan, 2004; Harp, Bressler, & Whitney 2007; McGraw, Levi, & Whitaker, 1999; Mussap & Prins, 2002; Nishida & Johnston, 1999; Pavan & Mather, 2008; Ramachandran & Anstis, 1990; Snowden, 1998; Whitaker, McGraw, & Pearson, 1999; Whitney, 2002; Whitney & Cavanagh, 2000; Whitney & Cavanagh, 2003; Zanker, Quenzer, & Fahle, 2001). Adaptation to motion produces substantial shifts in the perceived position of subsequently viewed stationary patterns (see McGraw, Walsh, & Barrett, 2004; McGraw, Whitaker, Skillen, & Chung, 2002; Nishida & Johnston, 1999; Snowden, 1998).

An important question concerns the roles played by the two low-level motion processing stages (i.e., local detection of motion signals in V1 and integration of local signals in MT) in generating MIPS. McGraw et al. (2004) used transcranial magnetic stimulation (TMS) to disrupt cortical activity after motion adaptation. They found that the perceived offset in spatial position following adaptation was reduced when TMS was applied to MT, but not when it was applied to V1. Mussap and Prins (2002) reported that the apparent location of a patch of coherently moving dots was shifted in a manner that suggested the involvement of cooperative interactions during motion integration. In the present paper we used plaid patterns in a psychophysical procedure to investigate whether motion integration in MT is important in the generation of MIPS prior to adaptation. We compared position shifts induced by Gabor patches containing single grating components to position shifts induced by Gabor patches containing two-component plaids. If local motion signals in V1 influence perceived position, MIPS from plaids should reflect these signals. One possibility is that the MIPS generated by a plaid will be equal to the largest shift generated by its components. Alternatively, since two separate component MIPSs would be spatially superimposed in a plaid, the resultant MIPS might be equal to the averaged position of the MIPSs generated

* Corresponding author.
E-mail address: g.mather@susx.ac.uk (G. Mather).

0042-6989/$ - see front matter © 2009 Elsevier Ltd. All rights reserved.
doi:10.1016/j.visres.2009.07.016

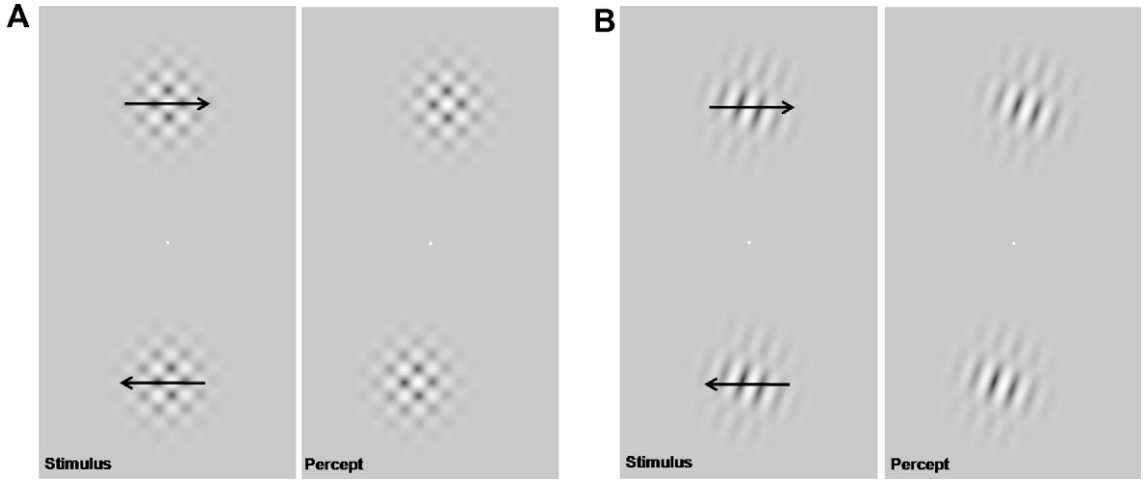

Fig. 1. (A) Stimulus and percept for Type I plaids. (B) Stimulus and percept for Type II plaids (see Method of Experiment 2 for further details about Type I and Type II plaids). The pictures show an example in which the two plaids are physically aligned (we did not include such a condition in our experiments; see Method) but when both Type I plaids (A) and Type II plaids (B) drift in opposite directions they appear misaligned.

by the single components. On the other hand, if the motion signals that influence perceived position reflect MT output, then MIPS from plaids should be consistent with predictions from motion integration computations on the components (Adelson & Movshon, 1982; Wilson & Kim, 1994). The first experiment measured MIPS from individual component gratings, and the second experiment measured MIPS from plaids containing pairs of these components. Results from the component MIPS experiment were used to generate predictions for the MIPSs obtained using plaids, in order to establish the cortical origin of the motion signals that influence perceived position.

2. Experiment 1: MIPS from individual gratings

The purpose of Experiment 1 was to measure the MIPS from individual grating components (consisting of drifting Gabors). The same components will be used in Experiment 2 to generate plaid patterns, so the results of Experiment 1 will be used to generate predictions for the MIPSs using plaids.

2.1. Method

2.1.1. Subjects

Two authors and six subjects who were unaware of the purpose of the study participated. All subjects had normal or corrected-to-normal visual acuity.

2.1.2. Apparatus

Stimuli were generated by a CRS VSG2/5 graphics system and displayed on a Sony Trinitron G400 monitor with a refresh rate of 100 Hz. The screen resolution was set to 1024×768 pixels. The mean background luminance was 29.03 cd/m^2, and the maximum and minimum luminances were 60.67 cd/m^2 and 0.007 cd/m^2 respectively. Luminance was measured using a Minolta LS-100 photometer. A gamma-corrected lookup table (LUT) was used to ensure stimulus linearity.

2.1.3. Stimuli

Visual stimuli were single-component Gabor patches drifting at the directions and velocities shown in Table 1. These component directions and velocities were selected because they can be used in later experiments to create Type I and Type II plaids.

Each Gabor consisted of a sinusoidal grating modulated by a static Gaussian. The Gabors had a full width of 3.5° at half maximum amplitude. Formally the Gabors can be defined as:

$$G_{(x,y,t)} = \sin[2\pi f_s(\cos\theta X + \sin\theta Y) + 2\pi f_t t + \phi]e^{-\frac{(x^2+y^2)}{\sigma^2}} \quad (1)$$

where $G_{(x,y,t)}$ represents the luminance at each point of the stimulus at the instant t, the contrast of the Gabors was always at 1 (Michelson contrast), ϕ is the phase shift of the sinusoidal carrier, f_s is the spatial frequency (1 c/deg) of the sinusoidal carrier, f_t is the temporal frequency of the sinusoidal carrier, θ is the orientation of the Gabor patch (conventionally 90° corresponds to horizontal drift of a vertical grating), and X, Y represent respectively the horizontal and vertical dimensions of the sinewave grating. The Gaussian envelope is expressed by the exponential of Eq. (1); x and y represent the respective horizontal and vertical distances from the Gaussian peak, σ is the space constant of the Gaussian (1.78°). The Gaussian envelope was always static, whereas the sine wave drifted either at 16.7, 11.11 or 5.5 deg/s.

2.1.4. Procedure

Subjects sat in a dark room and their head was immobilized with a chin rest placed at 57 cm from the screen. Viewing was binocular. Subjects were instructed to fixate a point at the centre of the screen and were given training at the beginning of each experiment to familiarise them with the stimuli and task. They were required to report the apparent relative horizontal position of two Gabor patches placed 10.18° above and 10.18° below the fixation point. On each trial the two Gabors contained gratings at the same orientation, drifting at the same velocity but in opposite directions. All of the components reported in Table 1 generate a rightward motion direction, however, half of the stimuli presented in the actual experiment (randomly selected from trial to trial) were made up by components generating a leftward motion direction (not

Table 1
Direction and velocity used for each component in Experiment 1.

Direction (deg)	Velocity (deg/s)
0	16.7
48.2	11.11
311.8	11.11
70.5	5.5

shown in Table 1: components at 180°, 132°, 229°, 109.5°, and drifting respectively at 16.7, 11.11, 11.11, and 5.5 deg/s).

On each trial the two Gabors were presented horizontally offset in opposite directions with respect to the fixation point by one of six values (−0.71°, −0.43°, −0.14°, 0.14°, 0.43°, 0.71°; positive values indicate rightward offset, negative values indicate leftward offset). There were a total of 24 conditions: 4 (component orientations) × 6 (horizontal offsets). Forty trials were performed for each condition, resulting in 960 trials. The order of conditions was randomized according to the Method of Constant Stimuli. Each stimulus was presented for 500 ms, after which the subject indicated with a button press whether the top Gabor appeared to be displaced to the left or to the right of the bottom one. A logistic function was fitted to the data in order to estimate the 50% point corresponding to the physical misalignment between the Gabors required for apparent alignment (the point of subjective equality or PSE; Finney, 1971; McKee, Klein, & Teller, 1985).

2.2. Results and discussion

Mean MIPS from each component is shown in Fig. 2. The fastest horizontal component (i.e., the component at 0°) generated the largest position shift (0.27°), the equally oblique components at 48.2° and 311.8° generated near-identical position shifts of 0.13° and 0.12° respectively, whereas the component at 70.5° shifted perceived position by 0.06°. A repeated measures ANOVA revealed a significant effect of component velocity/orientation ($F_{1,7} = 8.02$, $P = 0.001$). Pairwise comparisons showed that the component at 0° produced a significantly higher shift in position than the component at 48.2° ($P = 0.021$), a higher shift than the component at 311.8° ($P = 0.012$) and also a higher shift than the component at 70.5° ($P = 0.001$). However, we did not find significant differences between the components drifting at 48.2°, 311.8° and 70.5° ($P > 0.05$).

Subjects were instructed to judge the relative **horizontal** positions of the Gabor patches. Assuming that position shift is approximately proportional to drift velocity (as shown by the psychophysical data in Chung et al., 2007), it is possible to make a prediction for the horizontal component of the position shift of the obliquely moving components based on the position shift of the horizontally moving (vertical) component. Thus, a tilted component should generate a position shift equal to:

$$S = Shift_0[(V_c/V_0)\cos\theta_c] \quad (2)$$

where S is the position shift obtained using the tilted grating, $Shift_0$ is the position shift obtained for the vertical component, V_c is the velocity (deg/s) of the tilted component, V_0 is the velocity (deg/s) of the vertical component and θ_c is the orientation of the tilted component. For example, the component at 48.2° should produce a position shift of $0.27 * [(11.11/16.7) * \cos(48.2)]$, that is 0.12° (i.e., 0.44 times the position shift at 0°).

These predictions are shown by the black bars in Fig. 2, and offer a good account of the data except for some under-estimation of the effect at the slowest velocity. A repeated measures ANOVA conducted on the slopes of the best-fitting psychometric functions did not reveal a significant effect of component velocity ($F_{1,7} = 2.67$, $P > 0.05$) (mean slopes: 0.0082°, 0.0065°, 0.0071° and 0.0067° respectively for component at 0°, 48.2°, 311.8° and 70.5°, SEM: 0.0004, 0.0009, 0.0007, 0.0006 respectively for component at 0°, 48.2°, 311.8° and 70.5°). The absence of a significant difference between the slopes indicates that there were no differences in subjects' ability to discriminate small differences in position for different stimuli.

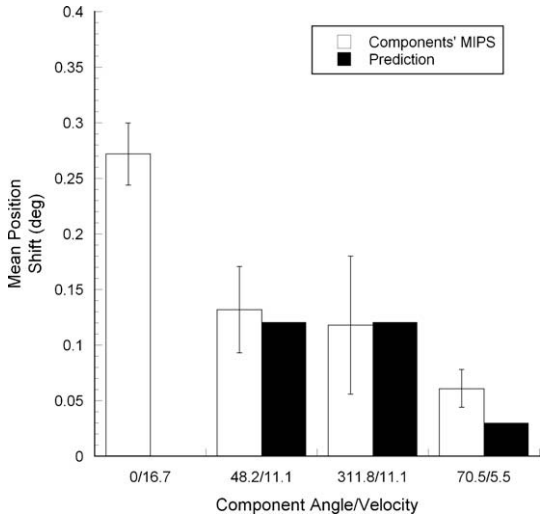

Fig. 2. Mean position shift obtained in Experiment 1 for each component ($N = 8$). Bars show the mean PSE, estimated by fitting a Logistic function to each subject's psychometric function in each condition. The component at 0° produced the largest effect (0.27°). Black bars indicate the predicted position shifts calculated on the basis of the MIPS obtained for the component at 0° (see text and Eq. (2) for more details). Error bars ± SEM.

3. Experiment 2: MIPS from plaids

Pairs of the components used in Experiment 1 were used to create two plaid patterns (i.e., Type I and Type II plaids), which give different predicted plaid directions according to two popular models of motion integration in plaids: the intersection-of-constraints (IOC) solution and the vector-sum (VS) solution (predictions were computed using the methods described in Bowns, 1996). The use of both Type I and Type II plaids allows us to investigate which integration mechanism, if any, is relevant to MIPS. The reasoning was that if motion signals generated in V1 influence perceived position, then MIPSs from plaids should reflect these signals. As described earlier, plaid MIPS may be equal to the largest shift generated by its components. Alternatively, plaid MIPS may be equal to the average of the MIPSs generated by the single components. However, if motion signals generated in MT contribute to perceived position, then MIPSs from plaid patterns should be larger than the component MIPSs, in accord with predictions from IOC or VS computations on the components (or some combination of the two).

3.1. Method

3.1.1. Subjects

Two authors and a new sample of six subjects who were unaware of the purpose of the study participated.

3.1.2. Apparatus

The apparatus was the same as that used in Experiment 1.

3.1.3. Stimuli

Visual stimuli in Experiment 2 were plaid patterns obtained by combining the components used in Experiment 1. Components at 48.2° and 311.8° were combined to create a Type I plaid. In this case both IOC and VS solutions lie inside the included angle between the components (Fig. 3A); both these solutions predict that the resultant plaid pattern drifts horizontally (Fig. 3A). Components at 70.5° and 48.2° were combined to create a Type II plaid. In this case the IOC solution lies outside the included angle between the components, but the VS solution lies inside the included angle (see Fig. 3B); IOC and VS solutions predict different drift directions for Type II plaids, that is, horizontally (0°) for the IOC

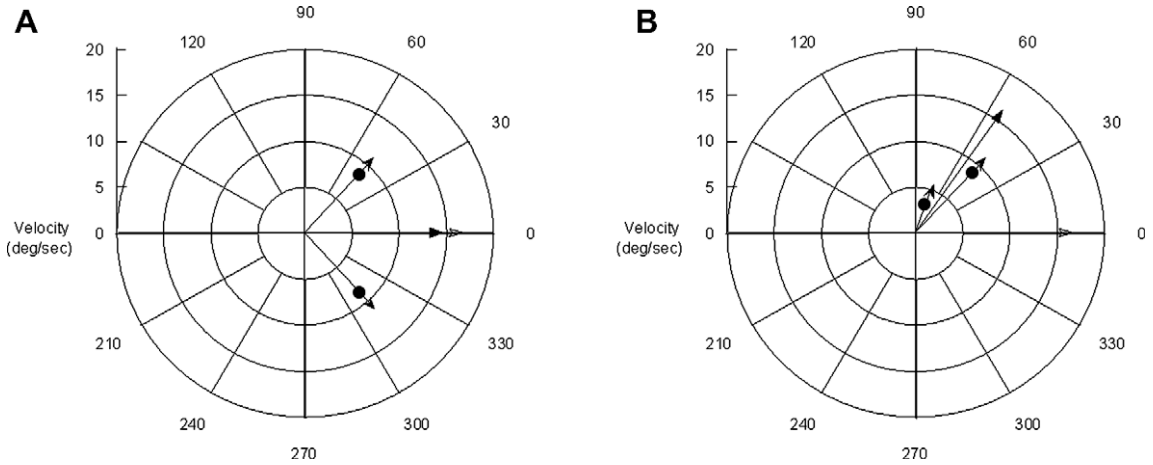

Fig. 3. Vector plot of the components used in Experiment 2 to create Type I (A) and Type II (B) plaids. To obtain a Type I plaid (A) components drifted at 48.2° and 311.8° (the components are marked with full circles). A Type II plaid (B) was created by combining components drifting at 70.5° and 48.5°. The vector plot also shows the resultant direction of the plaid patterns (thick black arrows) consistent with predictions from a motion integration computation on the components, i.e., vector-sum (VS) and intersection-of-constraints (IOC). See text for more details.

solution, and 55.54° for VS solution. Type I and Type II plaids drifted at a constant velocity of 16.7 deg/s, the same velocity as the component at 0° in Experiment 1; this allows us to calculate the predicted MIPS for plaid patterns from the MIPS obtained for the fastest component in Experiment 1 (i.e., the component at 0°).

Formally Type I and Type II plaids can be described as:

$$P_{(x,y,t)} = \left\{ \sin\left[2\pi f_s(\cos\theta_1 X + \sin\theta_1 Y) + 2\pi f_{t1} t + \phi_1\right] e^{-\frac{(x^2+y^2)}{\sigma^2}} + \sin\left[2\pi f_s(\cos\theta_2 X + \sin\theta_2 Y) + 2\pi f_{t2} t + \phi_2\right] e^{-\frac{(x^2+y^2)}{\sigma^2}} \right\} / 2C \qquad (3)$$

where $P_{(x,y,t)}$ represents the luminance at each point of the plaid at the instant t, ϕ_1 and ϕ_2 represent the phase shifts of the two sinusoidal carriers, f_s is the spatial frequency (1 c/deg) of the sinusoidal carriers, f_{t1} is the temporal frequency of the first component (i.e., 11.11 and 5.5 Hz for Type I and Type II plaids respectively), f_{t2} is the temporal frequency of the second component (i.e., 11.11 Hz for both Type I and Type II plaids), θ_1 is the orientation of the first component (i.e., giving directions of 48.2° and 70.5° for Type I and Type II plaids respectively), θ_2 represents the orientation of the second component of the plaid (i.e., giving directions of 311.8° and 48.2° for Type I and Type II plaids respectively), X, Y represent the horizontal and vertical dimensions of the sinewave grating of each component and C represents the Michelson contrast of the plaid pattern. The Gaussian envelope of each component is expressed by the exponentials in the Eq. (3), and was the same as that used in Experiment 1.

3.1.4. Procedure

The procedure in Experiment 2 was similar to that used in Experiment 1. Subjects fixated a point at the centre of the screen and judged the relative horizontal position of two plaid patterns placed at 10.18° above and 10.18° below the fixation point. On any one trial the plaid patterns were both Type I or both Type II plaids and always drifted in opposite directions, and were horizontally offset in opposite directions with respect to the fixation point by one of six values (−0.71°, −0.43°, −0.14°, 0.14°, 0.43°, 0.71° of visual angle; positive values indicate rightward offset, negative values indicate leftward offset). There were a total of 12 conditions: 2 (plaid types) × 6 (horizontal offsets). Forty trials were performed for each condition, resulting in 480 trials. The order of conditions was randomized. Each display was presented for 500 ms, after which the subject indicated with a button press whether the top Gabor appeared more to the left or more to the right of the bottom one. As in Experiment 1, a logistic function was fitted to the data in order to estimate the 50% corresponding to the physical misalignment between the plaids required for apparent alignment.

3.2. Results

Results showed that both Type I and Type II plaids shifted in apparent position towards the direction of motion. Thus, if plaids are physically aligned (Fig. 1A and B, left), they appear shifted towards the patterns' motion directions (Fig. 1A and B, right).

Fig. 4 shows the mean position shift generated by Type I and Type II plaids (dark grey bars), and the predicted MIPS (grey,

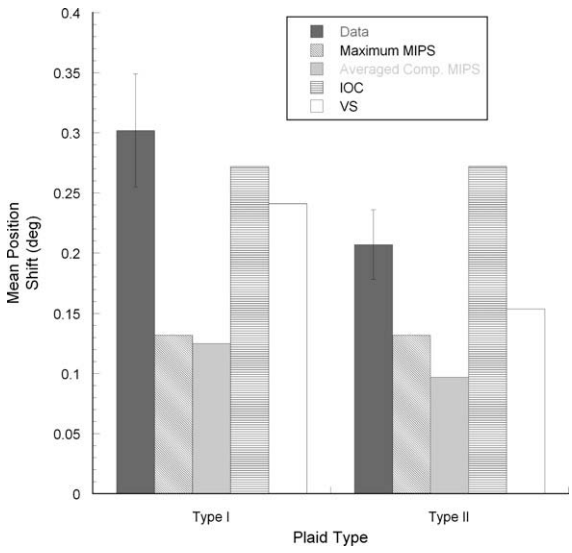

Fig. 4. Mean position shift for Type I and Type II plaids obtained in Experiment 2, and predictions of alternative accounts. Dark grey bars show the mean position shift obtained for Type I and Type II plaids. The shift obtained for Type I plaids is significantly higher than that found for Type II plaids, $P = 0.016$). Oblique hatched bars represent the MIPS predicted from averaging the MIPSs obtained for each component in Experiment 1, and light grey bars represent the maximum component MIPS obtained in Experiment 1. Horizontal hatched and unfilled bars show predicted MIPS calculated from the IOC and VS solutions, using results for the vertical component in Experiment 1. See text for more details. Error bars ± SEM.

hatched and unfilled bars) calculated from the MIPS produced in Experiment 1 according to the different accounts of the cortical origin of the motion signals. Oblique hatched bars represent the MIPS expected by averaging the MIPSs obtained for components at 48.2° (0.13°) and 311.8° (0.12°) in the case of Type I plaids (MIPS predicted: 0.125°), and the MIPS expected by averaging the MIPSs obtained for components at 48.2° (0.13°) and 70.5° (0.06°) in the case of Type II plaids (MIPS predicted: 0.095°). Light grey bars represent the maximum MIPS obtained for the relevant components in Experiment 1 (i.e., the components at 48.2°; MIPS: 0.13°). Horizontal hatched and unfilled bars show predicted MIPS according to the IOC and VS computations respectively. To illustrate how the predictions were derived, consider the Type II plaid. To predict the MIPS derived from a VS computation, we first compute the VS direction and velocity (55.54° and 16.3 deg/s), and then use these values to compute MIPS according to Eq. (2): $0.27 * [(16.3/16.7) * \cos(55.54)] = 0.14°$. To predict the MIPS derived from an IOC computation, we first compute IOC direction and velocity (0° and 16.3 deg/s), and again compute MIPS from Eq. (2): $0.27 * \cos(0) = 0.27°$. These predictions are shown in Fig. 4; The Type II MIPS prediction for the IOC solution in Experiment 2 corresponds to the position shift found for the 0° component in Experiment 1, since both move horizontally. The Type II MIPS prediction for the oblique VS solution in Experiment 2 is re-scaled to reflect the horizontal component of velocity (in the same way as the predictions in Experiment 1 were re-scaled).

Inspection of the graph shows that the obtained position shift for Type II plaids (0.20°) was smaller than the position shift obtained for Type I plaids ($F_{1,7} = 9.88$, $P = 0.016$), and intermediate between IOC and VS solutions.

A repeated measures ANOVA conducted on the slopes of the best-fitting psychometric functions for the plaids revealed no significant difference between Type I and Type II plaids ($F_{1,7} = 1.41$, $P > 0.05$), for which the mean slopes were 0.0079° and 0.008° respectively (SEM: 0.0003 and 0.0004 respectively for Type I and Type II plaids). The absence of a significant difference between the slopes indicates that there were no differences in subjects' ability to discriminate small differences in plaid position.

3.3. Discussion

Comparing predictions and data, Fig. 4 shows that position shifts in Experiment 2 are clearly much higher than those predicted simply by taking the average or the maximum of the component shifts, so we infer that the plaid position shifts reflect the output of an integration mechanism. For Type I plaids the obtained position shift lies close to the (very similar) predictions of both IOC and VS solutions (0.30°). For Type II plaids the obtained position shift lies intermediate between the predictions of the IOC and VS solutions. This may reflect the fact that the apparent motion direction of a Type II plaid was itself intermediate between the predictions of the two solutions (as found previously by, for example, Bowns, 1996; Bowns & Alais, 2006; Yo & Wilson, 1992), rather than in close alignment with only one or the other. To test this explanation, we conducted a third experiment to measure and match the apparent directions of the two types of plaid.

4. Experiment 3: adjusting plaids for apparent direction

Since the MIPS obtained in Experiment 2 for Type II plaids was intermediate between the IOC and VS predictions, we hypothesised that the apparent motion direction of the Type II plaid was intermediate between the directions predicted by IOC and VS solutions. We therefore conducted a third experiment to measure the apparent directions of Type I and Type II plaids. We then measured the position shift induced by the plaids using the same technique as in Experiment 2, this time after rotating the plaids individually for each subject so that their apparent direction was always horizontal. If the difference between the position shifts for Type I and Type II plaids in Experiment 2 was due to their different apparent motion directions, then once the plaids have been rotated so that they all appear to move horizontally the shifts obtained from Type I and Type II plaids should be equal (since the lengths of the vectors computed by the IOC and VS solutions are equal).

4.1. Method

4.1.1. Subjects

One author and a new sample of seven subjects who were unaware of the purpose of the study participated.

4.1.2. Apparatus and procedure

All methodological details concerning apparatus, stimuli and procedure were the same as in previous experiments, with the following exceptions.

In the first part of Experiment 3 we measured the apparent motion direction of Type I and Type II plaids. Plaids were computed as described in Experiment 2; they had a full width of 3.5° and always drifted in opposite directions at a constant velocity of 16.7 deg/s. Subjects fixated a point at the centre of the screen; two plaids were presented at 10.18° above and 10.18° below the fixation point. Apparent motion direction was measured separately for Type I and Type II plaids, as follows. A line with a full length of 16° of visual angle crossed the fixation point so that the centre of the line and the fixation point overlapped. On each trial the line was tilted at one of six values: 0°, 359°, 358°, 357°, 356° and 355° for Type I plaid; or 0°, 10°, 20°, 30°, 40° and 50° for Type II plaids (these values were chosen on the basis of pilot observations). Line orientation varied randomly from trial to trial according to the Method of Constant Stimuli. Each display was presented for 500 ms, after which the subject indicated with a button press whether the line was tilted clockwise or counterclockwise with respect to the motion direction of the two plaids. Subjects performed 240 trials for each plaid type. As before, a logistic function was fitted to the data in order to estimate the 50% point corresponding to the physical orientation of the line required for apparent alignment with the apparent direction of the plaids.

In the second part of Experiment 3 were measured the position shift induced by Type I and Type II plaids, using the same technique as in Experiment 2, with the difference that the plaids were rotated individually for each subject on the basis of the PSE values estimated in phase one of the Experiment, so that the apparent direction of the plaids was always horizontal.

4.2. Results and discussion

The results of the first part of Experiment 3 showed that the apparent direction of Type II plaids was much more oblique than the apparent direction of Type I plaids. Indeed, to render the apparent direction of the plaids horizontal it was necessary to rotate them clockwise by 1.8° and 40.6°, respectively for Type I and Type II plaids (SEM: 0.3 and 2.5 respectively for Type I and Type II plaids).

Using plaids that were adjusted so that they appeared to move horizontally, we did not find any significant difference between the position shifts obtained for Type I (0.29°) and Type II plaids (0.26°) ($F_{1,7} = 1.10$; $P > 0.05$) (Fig. 5). Moreover, these position shifts are not significantly different from the position shift obtained with Type I plaids in Experiment 2 (0.30°) ($F_{1,7} = 0.23$; $P > 0.05$). These results suggest that position shifts seen using plaid patterns reflect an integration mechanism that includes contributions from both IOC and VS computations.

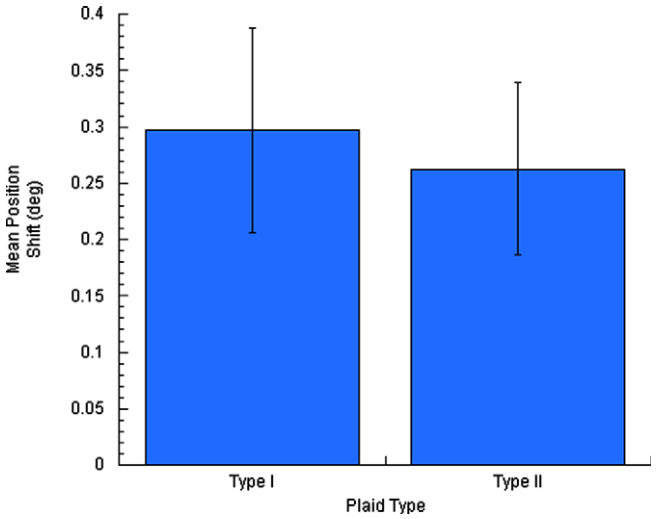

Fig. 5. Perceived misalignment for Type I and Type II plaids in Experiment 3, in which the plaids were rotated to obtain an apparent horizontal motion direction. There was no significant difference between the MIPS obtained for Type I plaids (i.e., 0.29°) and the MIPS obtained for Type II plaids (i.e., 0.26°) ($F_{(1,7)} = 1.10$; $P > 0.05$). In addition a repeated measures ANOVA showed no significant differences between the position shifts for Type I plaids obtained in Experiment 2 and the position shifts found for Type I and Type II plaids in Experiment 3 ($F_{(1,7)} = 0.23$; $P > 0.05$). Error bars ± SEM.

A repeated measures ANOVA did not show any significant difference between the best-fitting slopes for Type I (mean: 0.0081°, SEM: 0.00077) and Type II plaids (mean: 0.0083°, SEM: 0.00066) ($F_{1,7} = 0.32$; $P > 0.05$). Moreover, the slopes calculated in Experiment 3 were not significantly different from the slope calculated for Type I plaids in Experiment 2 (mean: 0.0079°, SEM: 0.0003) ($F_{1,7} = 0.22$; $P > 0.05$). This suggests that after the adjustment of the plaid motion direction, position sensitivity is equal for Type I and Type II plaids.

5. General discussion and conclusions

The results of these three experiments show that the motion signals giving rise to MIPS originate at or after the point at which local motion sensor outputs are integrated, rather than before. These results are therefore consistent with those of McGraw et al. (2004) and Mussap and Prins (2002) described earlier. We concur with McGraw et al.'s (2004) conclusion that the anatomical locus of interaction between motion and position signals is area MT. McGraw et al. (2004) suggest that information about local features is lost during motion and position interactions. However, in another recent paper (Pavan & Mather, 2008) we reported that MIPS respects the distinction between first-order and second-order motion, so some featural information is preserved during the computations mediating MIPS.

MIPSs in plaids are larger than expected on the basis of shifts in individual components, and are consistent with an integration mechanism that combines IOC and VS computations. Such a mechanism has been proposed in other studies of motion perception in plaids (e.g., Bowns & Alais, 2006; Yo & Wilson, 1992). A VS computation is required to explain our MIPS data even though the duration of our stimulus exceeded that normally associated with VS effects. Adaptation effects reported by Bowns and Alais (2006) indicate that the VS direction is not simply a transient phase during integrative computations, but a viable steady-state solution. Perhaps the interactions mediating position shifts place more weight on the VS computation rather than the IOC computation. Note that there is no evidence to support a vector average computation, which would predict a relatively small position shift (similar, in fact, to the predictions for the component averages shown in Fig. 4). Instead, position shifts in plaids reflect the higher velocity given by a VS computation. It is not clear whether this VS effect is unique to MIPS interactions, or reflects a more general property of motion integration computations.

We conclude that MIPS is governed by the perceived direction of a plaid pattern, rather than the actual directions of its components, and arises during extrastriate processing in cortical area MT.

References

Adelson, E. H., & Bergen, J. R. (1985). Spatiotemporal energy models for the perception of motion. *Journal of the Optical Society of America A-Optics Image Science and Vision, A2*, 284–299.

Adelson, E. H., & Movshon, J. A. (1982). Phenomenal coherence of moving visual patterns. *Nature, 300*(5892), 523–525.

Bowns, L. (1996). Evidence for a feature tracking explanation of why Type II plaids move in the vector sum direction at short durations. *Vision Research, 36*(22), 3685–3694.

Bowns, L., & Alais, D. (2006). Large shifts in perceived motion direction reveal multiple global motion solutions. *Vision Research, 46*, 1170–1177.

Chung, S. T., Patel, S. S., Bedell, H. E., & Yilmaz, O. (2007). Spatial and temporal properties of the illusory motion-induced position shift for drifting stimuli. *Vision Research, 47*(2), 231–243.

De Valois, R. L., & De Valois, K. K. (1991). Vernier acuity with stationary moving Gabors. *Vision Research, 31*, 1619–1626.

Durant, S., & Johnston, A. (2004). Temporal dependence of local motion induced shifts in perceived position. *Vision Research, 44*(4), 357–366.

Durant, S., & Zanker, J. M. (2009). The movement of motion-defined contours can bias perceived position. *Biology Letters, 5*(2), 270–273.

Edwards, M., & Badcock, D. R. (2003). Motion distorts perceived depth. *Vision Research, 43*(17), 1799–1804.

Fang, F., & He, S. (2004). Strong influence of test patterns on the perception of motion aftereffect and position. *Journal of Vision, 4*(7), 637–642.

Finney, D. J. (1971). *Probit analysis*. Cambridge: Cambridge University Press.

Fu, Y. X., Shen, Y., Gao, H., & Dan, Y. (2004). Asymmetry in visual cortical circuits underlying motion-induced perceptual mislocalization. *Journal of Neuroscience, 24*(9), 2165–2171.

Harp, T. D., Bressler, D. W., & Whitney, D. (2007). Position shifts following crowded second-order motion adaptation reveal processing of local and global motion without awareness. *Journal of Vision, 7*(2), 1–13.

McGraw, P. V., Levi, D. M., & Whitaker, D. (1999). Spatial characteristics of the second-order visual pathway revealed by positional adaptation. *Nature Neuroscience, 2*(5), 479–484.

McGraw, P. V., Whitaker, D., Skillen, J., & Chung, S. T. L. (2002). Motion adaptation distorts perceived spatial position. *Current Biology, 12*, 2042–2047.

McGraw, P., Walsh, V., & Barrett, T. (2004). Motion-sensitive neurons in V5/MT modulate perceived spatial position. *Current Biology, 14*, 1090–1093.

McKee, S. P., Klein, S. A., & Teller, D. Y. (1985). Statistical properties of forced-choice psychometric functions: Implications of probit analysis. *Perception & Psychophysics, 37*(4), 286–298.

Mussap, A. J., & Prins, N. (2002). On the perceived location of global motion. *Vision Research, 42*(6), 761–769.

Nishida, S., & Johnston, A. (1999). Influence of motion signals on the perceived position of spatial pattern. *Nature, 397*(6720), 610–612.

Pantle, A., & Turano, K. (1992). Visual resolution of motion ambiguity with periodic luminance- and contrast-domain stimuli. *Vision Research, 32*, 2093–2106.

Pavan, A., & Mather, G. (2008). Distinct position assignment mechanisms revealed by cross-order motion. *Vision Research, 48*(21), 2260–2268.

Ramachandran, V. S., & Anstis, S. M. (1990). Illusory displacement of equiluminous kinetic edges. *Perception, 19*(5), 611–616.

Snowden, R. J. (1998). Shifts in perceived position following adaptation to visual motion. *Current Biology, 8*(24), 1343–1345.

Strout, J. J., Pantle, A., & Mills, S. L. (1994). An energy model of interframe interval effects in single-step apparent motion. *Vision Research, 34*, 3223–3240.

Whitaker, D., McGraw, P. V., & Pearson, S. (1999). Non-veridical size perception of expanding and contracting objects. *Vision Research, 39*(18), 2999–3009.

Whitney, D. (2002). The influence of visual motion on perceived position. *Trends Cognitive Sciences, 6*(5), 211–216.

Whitney, D., & Cavanagh, P. (2000). Motion distorts visual space: Shifting the perceived position of remote stationary objects. *Nature Neuroscience, 3*(9), 954–959.

Whitney, D., & Cavanagh, P. (2003). Motion adaptation shifts apparent position without the motion aftereffect. *Perception & Psychophysics, 65*(7), 1011–1018.

Wilson, H. R., & Kim, J. (1994). Perceived motion in the vector sum direction. *Vision Research, 34*(14), 1835–1842.

Yo, C., & Wilson, H. (1992). Perceived direction of moving two-dimensional patterns depends on duration, contrast, and eccentricity. *Vision Research, 32*(1), 135–147.

Zanker, J. M., Quenzer, T., & Fahle, M. (2001). Perceptual deformation induced by visual motion. *Naturwissenschaften, 88*(3), 129–132.